Ex-Core Thermo-Fluidics Optimization for Transformational Challenge Reactor

P. Vegendla[1a], A. Bergeron[a], M. Subhasish[a], A. Talamo[a], F. Heidet[a]
B. J. Ade[b], B.R. Betzler[b]

[a)]*Argonne National Laboratory, 9700 South Cass Avenue, Argonne, IL 60439, USA*
[b)]*Oak Ridge National Laboratory, P.O. Box 2008, Oak Ridge, TN 37831-6170, USA*
[1]svegendla@anl.gov

dx.doi.org/10.13182/T124-35232

INTRODUCTION

The safety of gas-cooled reactors must be ensured by active or passive cooling systems, which fulfill the task of keeping thermal loads on components and structures (i.e., vessel, confinement) within acceptable design limits under both normal and accident conditions. Thermo-fluidic computer codes help design, enhance performance and ensure a high safety level for these cooling systems [1, 2].

A computational fluid dynamics (CFD) model of the Transformational Challenge Reactor (TCR) [3] ex-vessel components and confinement was created to provide detailed information on the temperature distribution of ex-core components, such as vessel, shroud, reflectors and bio-shield. The TCR program uses a rapid additive manufacturing approach to design, build and operate a microreactor. The heat source values for these components were obtained from a detailed neutronic model of the TCR using Monte Carlo code MCNP [4]. Based on these neutronics simulations, it was estimated that about 3.4% of the total nuclear power is deposited ex-core (beyond the pressure vessel). If the in-core power is 3 MW, that represents about 102 kW deposited ex-core.

In our previous work [5] we concluded that an active ex-core air-cooling system is required to maintain the safety temperature limits for ex-core components.

Several 3D CFD simulations were performed to analyze the TCR ex-core temperature distribution for various ex-core airflow rates. STAR-CCM+® CFD commercial software was used to model thermo-fluidics phenomena, such as convective, conductive and radiative heat transfer. Simulation results were presented for three inlet coolant mass flow rates (2, 4 and 8 kg/s).

TABLE I. System operating conditions

Component	Value
RPV inside wall temperature [K]	573
Ex-core total heat source [kW]	102
Thermal specification for all walls, except floor	Environment
Ambient temperature [K]	300
Convective heat transfer coefficient [W/m^2-K]	20
Forced-air flow rate [kg/s]	2, 4 and 8

In this paper we present the numerical model of the ex-core/confinement of the TCR and the results of its forced-air cooling.

NUMERICAL MODELING

The vessel and its support structure (skirt) have been modeled explicitly and were directly imported from Oak Ridge National Laboratory's CAD model. The inner wall vessel temperature is fixed and a no-slip boundary condition is imposed for all walls. Heat is rejected from the containment building walls to ambient air with a provided convective heat transfer coefficient of 20 W/m^{2}K.

The ex-core geometry consists of several components: reactor pressure vessel (RPV), shroud, reflectors, concrete/bio-shield, heat exchanger and confinement walls. Stainless steel is used for modeling of all components except the bio-shield, which is blended cement. The assumed operating conditions and geometry details are given in Table I.

The axisymmetric CFD model created for the TCR confinement/ex-core simulations is shown in Figure 1. The heat exchanger is modeled as a porous body and considered 50% air and 50% steel volume fraction. The inertial and viscous flow resistance in the heat exchanger are set to zero.

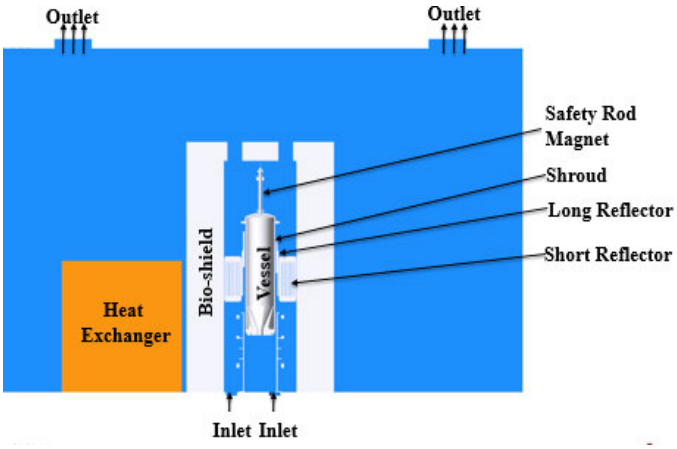

Fig. 1. Ex-core geometry configuration for forced-air cooling.

Three inlet coolant ducts are placed between both the RPV and the bio-shield, separated by an angle of 120°. The blower drives the specified air mass flow rate into the confinement from the three inlets. The hot air is removed via two vent/outlet ducts placed over the confinement roof.

The heat source distribution described in Section 3.1 of Bergeron et al. [6] is specified for all ex-core components except the heat exchanger (RPV, reflectors, shroud, bio-shield and support structures). The heat is removed via convection, conduction and thermal radiation. As shown in Table 3-2 of Bergeron et al. [6], the magnitude of the heat deposited in the ex-core components tends to be a function of the shroud position. Conservatively, the maximum power generated in each ex-core component between the two extreme cases, shroud in or out, has been selected. As a result, the total heat source deposited ex-core is 102 kW. While this approach may seem excessively conservative, it minimizes the risk of under dimensioning the ex-core cooling.

Modeled Details and Boundary Conditions

The STAR-CCM+ code uses the finite volume (FV) method to solve the Navier-Stokes fluid flow equations. In STAR-CCM+, the velocity and k-omega turbulence equations are solved using steady state, real gas, nonisothermal and segregated flow. Buoyancy effects are included by adding a gravity term. The grey thermal surface-to-surface radiative heat-transfer model was selected. The emissivity of the bio-shield and rest of the components are set at 0.94 and 0.8, respectively, which is considered a reasonable hypothesis. Temperature-dependent thermal-physical properties are implemented for both fluid and solid components, such as thermal conductivity, specific heat and density. To be noted, SS316 thermal properties are applied for all solid materials except bio-shield (concrete). The thermal properties of the SS316 can be found elsewhere [7]. The bio-shield density and specific heat are considered 2240 kg/m^3 and 654 J/kg.K^{-1}, respectively. The bio-shield variable thermal conductivities can be found elsewhere [8].

The operating conditions are presented in Table I. The environment boundary condition (ambient air temperature) is specified at the confinement walls except for on the ground floor. The convective heat transfer coefficient for the confinement wall boundaries is set at 20 W/m^{2}K, which is considered a reasonable hypothesis. For the RPV, a constant temperature boundary condition is specified for the inside wall (573 K). In addition, the conductive heat transfer boundary condition is specified for all support structures in direct contact with the ground floor.

In forced-air circulation, a pressure boundary condition was specified at the outlet, flow velocity and temperature were specified at inlet, and no-slip boundary condition was imposed at walls.

The volume mesh was generated to simulate the confinement configurations. The minimum volume edge size was 2 mm over the vessel, shroud and reflector surfaces and the maximum cell edge size was allowed to be as large as 60 mm near the confinement wall surfaces. In addition, three volumetric control blocks were introduced to control the mesh size around the bio-shield, reflector and shroud and vessel structures. This produces a finer mesh with a relatively uniform cell size, helping to prevent numerical instabilities. The maximum cell edge size was kept at 4.8 mm, 9.6 mm, 20 mm, respectively. A total of four prism layers with a total thickness of 2 mm were selected for all fluid-wall surfaces except for confinement and heat exchanger walls. The total generated mesh cells were close to 16 million. In addition, the mesh was refined approximately 1.2 times to ensure the present results are grid independent for calculated maximum temperatures in the bio-shield, reflectors and RPV (not shown due to negligible difference in relative errors <0.05%).

RESULTS

In order to understand the effect of the ex-core mass flow rate on the magnitude of the peak temperatures, three different calculations were tested where the flow rate was progressively increased from 2, 4 and then 8 kg/s. The results are provided for specified power distribution profiles for the RPV, shroud, reflectors, bio-shield and its support structures.

Figures 2–4 illustrate the results. Each figure is composed of three contour plots showing the results for the three cases (2, 4 and 8 kg/s). Figure 2 shows the velocity distribution, Figure 3 shows the temperature distribution and Figure 4 shows the temperature distribution in the solid region only.

This series of figures show, as expected, that the temperature in the ex-core components drops with an increase flow rate. However, the drop is not similar for all components. This is explained by two reasons:

- The component location (the farther away from the core tends to lower temperature). This is clearly visible on Figure 4, which shows the temperature in the shroud and long and short reflectors. The temperature in these components tends to decrease rapidly with increased distance from the core.
- The magnitude of the heat deposited in the component (tends to increase temperature). The increasing flow rate is more beneficial for the hotter components (shroud, long reflector) because the temperature drop is more significant.

The peak temperature and pressure drop are summarized in Table II. Based on the limited number of temperature limits defined, the shroud mechanisms appear to be the most limiting components, followed by the bio-shield (Figure 5). Figure 5 shows the peak temperature in these components as a function of flow rate. It can be seen

that a mass flow rate of 5 kg/s would be sufficient to cool down all components below their safety limits.

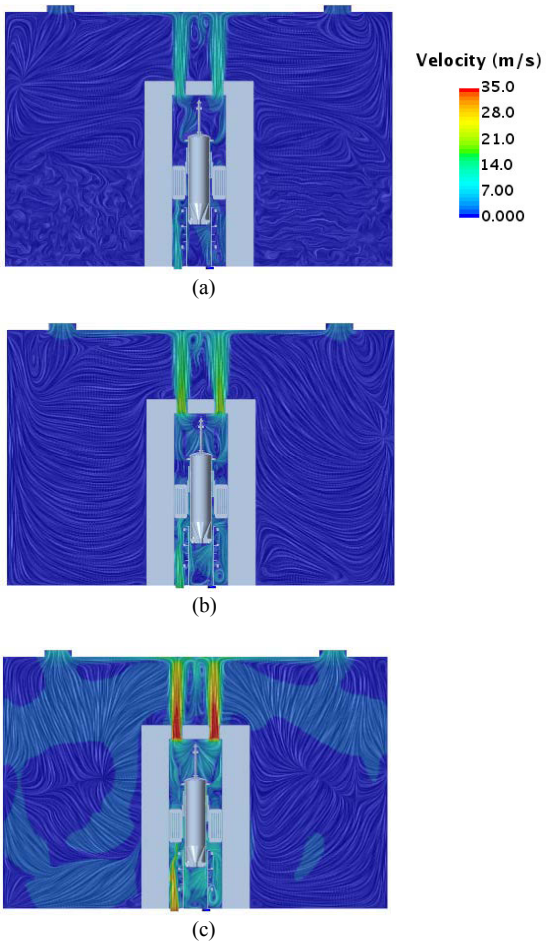

Fig. 2. Ex-core fluid velocity contours over XZ-plane. (a) 2 kg/s; (b) 4 kg/s; (c) 8 kg/s.

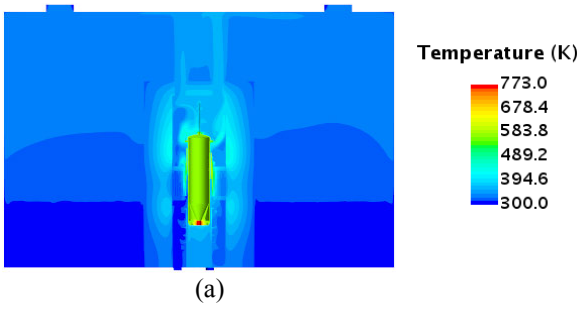

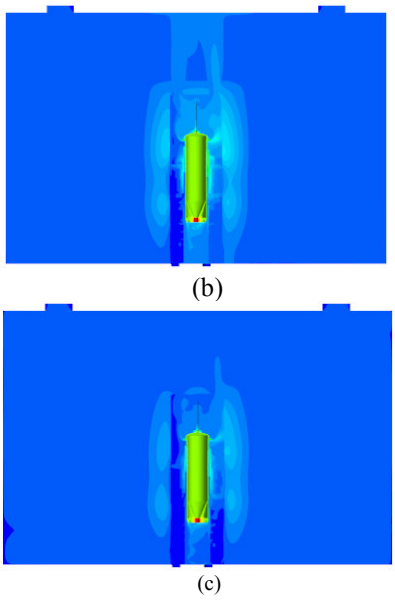

Fig. 3. Ex-core fluid and solid temperature distribution over axi-symmetric plane (XZ-plane). (a) 2 kg/s; (b) 4 kg/s; (c) 8 kg/s.

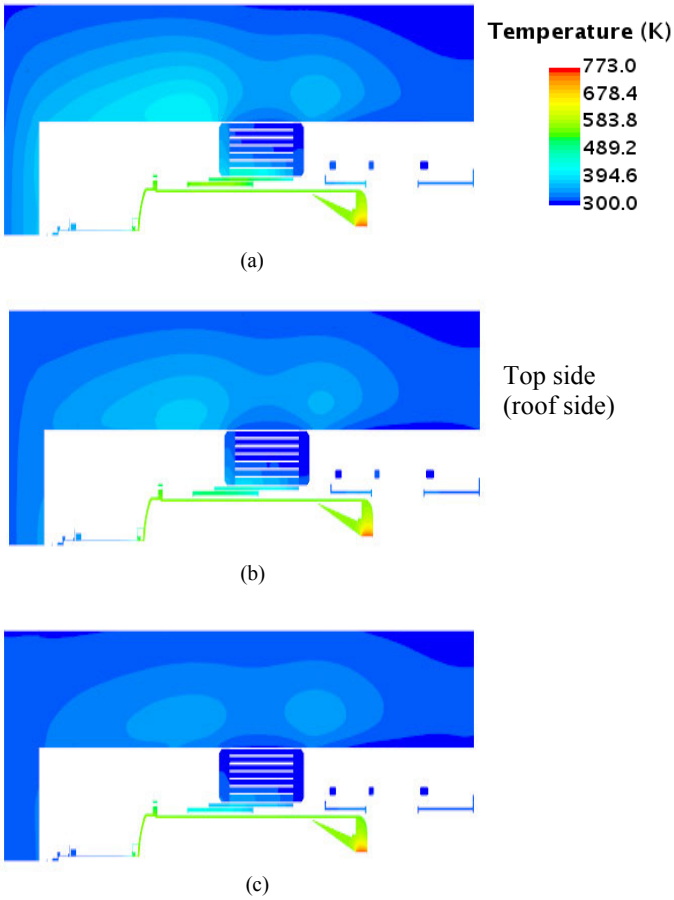

Fig. 4. Ex-core solid temperature distribution over vertical plane at center (YZ-plane) (rotated by 90°) for various inlet air coolant mass flow rates. (a) 2 kg/s; (b) 4kg/s; (c) 8 kg/s.

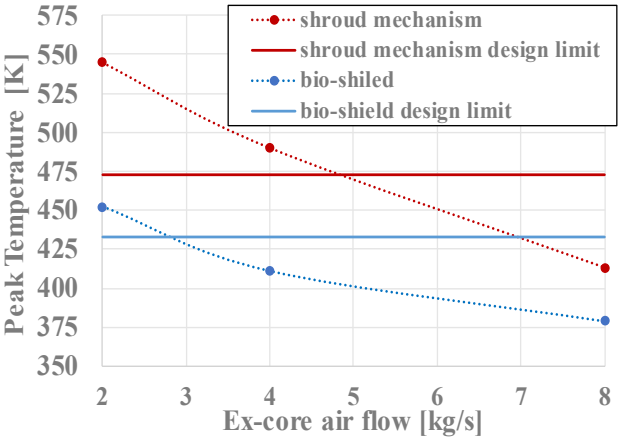

Fig. 5. Peak temperature in the bio-shield (blue dashed line) and shroud mechanisms (red dashed line) as a function of the air mass flow rate.

TABLE II. Ex-core temperature and pressure as a function of air flow

	Ex-core air flow (kg/s)			Design limit
	2	4	8	
Inlet temperature [K]		300		-
Outlet temperature [K]	338	324.7	316.9	-
Pressure drop [psi] (inlet-outlet)	0.032	0.096	0.28	-
Peak vessel temperature [K] in:				
Vessel	773 (boundary condition)			-
Shroud	611	542	473	-
Long reflector	590	506	437	-
Short reflector	517	440	384	-
Bio-shield	452	411	379	433
Safety rod	384	352	333	473
Shroud mechanism	545	490	413	473

CONCLUSIONS

3D CFD simulations were performed to optimize the ex-core airflow rate. The simulation results were presented for three different inlet coolant mass flow rates (2, 4 and 8 kg/s). The minimum flow rate sufficient to cool down all ex-core components considered below their safety limit was calculated to be 5 kg/s. The peak temperatures were within the safety limits for all components including bio-shield and shroud mechanism. Future work will involve the thermal optimization of new configurations for ex-core components due to continued evolution of TCR designs and its new requirements.

ACKNOWLEDGMENTS

The Transformational Challenge Reactor program is supported by the U.S. Department of Energy Office of Nuclear Energy (DOE-NE). The submitted manuscript has been created by UChicago Argonne, LLC, Operator of Argonne National Laboratory. Argonne National Laboratory's work was supported by the U.S. Department of Energy, Office of Nuclear Energy under contract DE-AC02-06CH11357.

REFERENCES

[1] E. Studer et al., "CAST3M/ARCTURUS: A coupled heat transfer CFD code for thermal-hydraulic analyses of gas cooled reactors," *Nuc. Eng. & Des.* 237: 1814–1828 (2007).

[2] C.H. Oh et al., *Development of Safety Analysis Codes and Experimental Validation for a Very High Temperature Gas-Cooled Reactor*, Idaho National Laboratory, INL/EXT-06-01362 (2006).

[3] K.A. Terrani, *Transformational Challenge Reactor Demonstration Program*, Oak Ridge National Laboratory (2019).

[4] C.J. Werner et al. (eds.), *MCNP6 User's Manual, Code Version 6.2*, Los Alamos National Laboratory, LA-UR-17-29981 (2017).

[5] P. Vegendla et al., "Ex-core thermo-fluid modeling and simulations for transformational challenge reactor," ANS-2020, American Nuclear Society (2020).

[6] A. Bergeron et al., Argonne National Laboratory, unpublished document (2020).

[7] K.G. Field et al., "Handbook of advanced manufactured material properties from TCR structure builds at ORNL-FY2019." ORNL/TM-2019/1328 (2019).

[8] Hyung et al. "Effective Thermal Conductivity and Diffusivity of Containment Wall for Nuclear Power Plant OPR1000", *Nuclear Energy and Design*, Volume 49(3), PP 459-465 (2017).